Organic–Inorganic Composite Materials from Acrylonitrile–Butadiene–Styrene Copolymers (ABS) and Silica through an *In Situ* Sol-Gel Process

YING GEV HSU, FUNG JUNG LIN

Department of Textile Engineering, National Taiwan University of Science and Technology, Taipei 10672, Taiwan, Republic of China

Received 9 September 1998; accepted 25 May 1999

ABSTRACT: Nonbonded and chemically bonded organic–inorganic composite materials, ABS/SiO_2 and ABS—$Si(OCH_3)_3/SiO_2$, were prepared by the sol-gel processing of tetraethoxysilane (TEOS) in the presence of ABS and trimethoxysilyl functionalized ABS, ABS—$Si(OCH_3)_3$, under the catalization of NH_4F. The ABS—$Si(OCH_3)_3$ was obtained by oxidizing the cyano group in ABS with hydrogen peroxide, then subsequently underwent ring-opening reaction with 3-glycidoxypropyltrimethoxysilane (GPTS). The ABS—$Si(OCH_3)_3$/TEOS sol-gel liquid solution system, in which the ABS chains formed the covalent bonds with silica network and helped fix the polymer chains in the silica network, had a shorter gelation time than that of the ABS/TEOS system, which linked ABS chains to the silica network only by hydrogen bonding the cyano groups in ABS to the silanol groups. The morphology and properties of composite were characterized by scanning electron microscopy (SEM), differential scanning calorimeter (DSC), tensile tests, and thermogravimetry. It was found that the composite prepared from ABS—$Si(OCH_3)_3$ had higher tensile strength, glass transition point (T_g), thermal stability, and more homogeneous morphology because of the existence of the covalent bond between ABS chains and silica network that increased the compatibility between the organic and inorganic phases. © 2000 John Wiley & Sons, Inc. J Appl Polym Sci 75: 275–283, 2000

Key words: acrylonitrile–butadiene–styrene copolymer (ABS); modified ABS; sol-gel process; silica network; interfacial force; organic–inorganic composite

INTRODUCTION

As a new class of materials, organic–inorganic sol-gel composite materials, synthesized through the synergistic combination of polymers and ceramics via sol-gel process, has recently attracted great attention in the field of materials science.[1–4] These materials combine the advantages of polymers, such as flexibility, toughness, and ease processing, with those of ceramics or glasses, such as hardness, durability, and thermal stability. In general, the largest area of organic–inorganic composite materials research activity has been inorganic modification of organic polymers, that is, the organic polymer is the dominant phase.[5,6] The polymers and ceramics are blended or reacted with each other by mutual dispersion at molecular level. The interfacial force between the organic and inorganic phases plays a major role in controlling the microstructures and the properties of the composite materials. Two approaches are normally utilized to establish this interfacial

Correspondence to: Y. G. Hsu.

Contract grant sponsor: National Science Council; contract grant number: NSC-86-2216-E-011-022.

Journal of Applied Polymer Science, Vol. 75, 275–283 (2000)

 CCC 0021-8995/00/020275-09

force.[7,8] In the first case, the polymer molecules are dispersed in the three-dimensional network of silica (or ceramic) by means of the formation of hydrogen bond between the basic group of the hydrogen acceptor in polymer and the silanol group (Si—OH) of the intermediate species from $Si(OR)_4$. The other case is the formation of a covalent bond between the polymer and silica. Polymers having —$Si(OR)_3$ groups at the end of polymer molecules or in the pendant groups are subjected to hydrolysis together with $Si(OR)_4$ in an homogeneous reaction system. Intermediate species of silanol groups derived from $Si(OR)_4$ and from —$Si(OR)_3$ in the polymer condense with each other to produce homogeneous materials consisting of chemically bonded components.

The acrylonitrile–butadiene–styrene copolymers (ABS) have frequently been chosen for commercial applications because of their excellent physical and mechanical properties, and the relatively low cost and ready availability of the required starting materials. The properties of this class of polymers can possibly be improved by incorporating a ceramic phase such as silica in it. In this article we have synthesized two types of organic–inorganic composite materials, ABS/SiO_2 and ABS—$Si(OCH_3)_3$/SiO_2, by the incorporating of silica in ABS matrix. For the ABS/SiO_2 composite, this was obtained by the sol-gel process of tetraethoxysilane (TEOS) in THF in the presence of ABS with hydrogen bonds as the interfacial force between ABS matrix and silica networks. On the other hand, the ABS—$Si(OCH_3)_3$/SiO_2 composite was synthesized by hydrolyzing and cocondensing of ABS—$Si(OCH_3)_3$, modified by the introduction of —$Si(OCH_3)_3$ groups in the ABS chains, with TEOS through the sol-gel process. The covalent bonds are formed between the ABS matrix and the silica. Because different catalysts produce significant variation in microstructure and the consequent properties of the composites, both types of composites were prepared under the catalyzation of NH_4F.[9,10] The properties of the resultant composites are reported and discussed in this article.

EXPERIMENTAL

Materials

TEOS was purchased from Acros Chemical Co. and was purified by distillation. 3-Glycidyloxypropyltrimethoxysilane (GPTS) was purchased from the Merck Chemical Co., and was used without further purification. ABS was generously supplied by Nan-Ya Plastic Co. Ltd. Other reagents were purified by conventional methods.

Preparation of Trimethoxysilyl-Functionalized ABS[11]

Into a three-necked round-bottomed 500-mL flask, equipped with a stirrer, a cooler, an N_2 inlet, 50.0 g of ABS, 30.0 mL of 35% H_2O_2 and 0.05 g of K_2CO_3 were dissolved in 400 mL of DMSO. The solution was then heated at 50°C for 12 h. At the end of the reaction the methanol/H_2O solution (v/v: 80/20) was added in the reaction mixture to precipitate the hydrolyzed product, M-ABS, and the product was washed with methanol/H_2O solution three times to remove K_2CO_3 and H_2O_2. The pure M-ABS was then obtained by redissolving the precipitate in THF, filtering the impurity followed by precipitating the filtrate with methanol for two times.

In a three-necked round-bottomed 500-mL flask, with the same equipment as described above, the pure product M-ABS was dissolved in 300 mL of toluene. Three grams of GPTS and a trace amount of triphenylphosphine (TPP) were added in the solution. The reaction mixture was then heated at 90°C for 12 h. The $Si(OCH_3)_3$ containing ABS, i.e., ABS—$Si(OCH_3)_3$, was obtained by the ring-opening reaction of GPTS with the carboxylic and amide groups in ABS. The scheme for the preparation of modified ABS was summarized in Scheme 1.

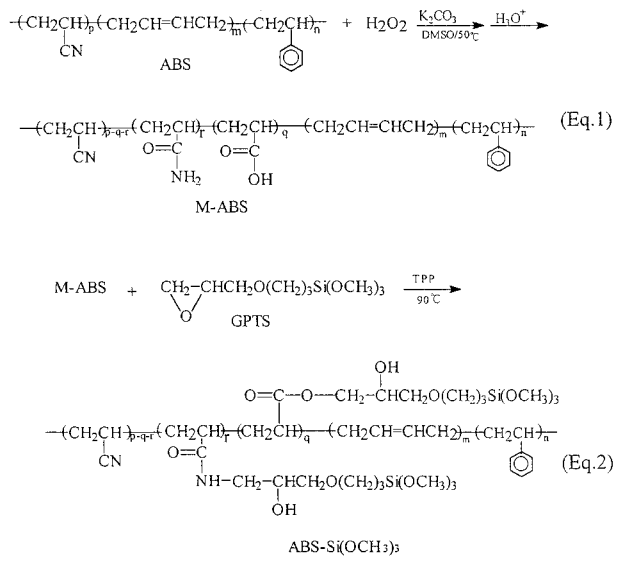

Scheme 1 The modification of ABS.

Table I Compositions of Various Sol-Gel Liquid Solutions of Composite Materials

	SiO_2 (wt %)	2.5	7	15	30
Sol A	ABS—$Si(OCH_3)_3$ or ABS (g)	3.75	3.37	2.63	1.05
	THF (g)[a]	6.06	6.30	6.30	3.90
Sol B	TEOS (g)	0.33	0.81	1.62	1.56
	THF (g)[a]	1.56	1.56	1.42	0.96
	$[H_2O]/[TEOS]$[b]	2.2	2.2	2.2	2.2
	$[NH_4F]/[TEOS]$[b]	0.016	0.016	0.016	0.016

[a] The total amount of THF in sol-gel liquid solution was 65 wt %.
[b] The mol ratio of H_2O and NH_4F with TEOS.

At the end of reaction, methanol was added in the reaction mixture to precipitate the product. The pure ABS—$Si(OCH_3)_3$ was then obtained by redissolving the precipitate in THF, filtering the impurity, and then precipitating the filtrate with methanol for two times. The structure and molecular weight of the modified ABS was determined by FTIR, thermogravimetry analyzer, and GPC.

Preparation of Nonbonded ABS/SiO_2 Composite Materials

The stoichiometric amount of TEOS, H_2O, and NH_4F were dissolved in THF (Table I). The mixture was stirred at room temperature for 30 min to obtain a homogeneous solution called Sol B. Sol B was then combined with the THF solution of ABS (Sol A). The mixture of Sol A and Sol B was then stirred for another 10 min. This homogeneous mixture was subsequently used to prepare the nonbonded ABS/SiO_2 composite materials through the sol-gel process. Films of ABS/SiO_2 composite material of uniform thickness were obtained by casting the sol-gel solution onto a plate, which was then sealed for gelling at 30°C. The time required for gelation (i.e., gelation time) was taken to be that at which there was no further visible flow. The resultant gels were dried slowly in air at the same temperature for a period of time (from several days to 1 month) until the sample reached a constant weight.

Preparation of Chemically Bonded ABS—$Si(OCH_3)_3/SiO_2$ Composite Materials

Sol B was prepared according to the recipes listed in Table I, and was added slowly into the THF solution of ABS—$Si(OCH_3)_3$ (sol A) to form an homogeneous sol-gel liquid solution. The sol-gel liquid solution was subsequently used to prepare the chemically bonded composite materials, ABS—$Si(OCH_3)_3/SiO_2$, through the sol-gel process. The preparation conditions of the materials were the same as those described above.

Measurements

IR spectra of ABS and modified ABS, including M-ABS and ABS—$Si(OCH_3)_3$, were recorded with a Bio-Rad SPC-3200 FTIR (Japan). Samples for FTIR were prepared by coating the polymer on KBr disks. The molecular weight of ABS and ABS—$Si(OCH_3)_3$ were measured using LC-500 GPC (GL Sciences Inc., Japan) with the operation conditions as following: column, Pigel 5 μ Mixed-D 7.5 $\times$ 300 mm; solvent, THF; concentration, 0.1 g/100 mL; flow rate, 0.8 L/min; temperature, 40°C; Detector, RI. The morphology of the materials were observed by a scanning electron microscopy (SEM Cambridge S 360, UK). The glass transition point (T_g) of the composites were determined with a differential scanning calorimetry (DSC, DuPont 2100) under an N_2 flow, with a heating rate of 20°C min^{-1}. The initial decomposition point (IDT) of the composites were determined with thermogravimetry analyzer (TGA, DuPont 2100) under an N_2 flow, with the heating rate of 10°C min^{-1}. Tensile strengths of the hybrids were measured using an Instron instrument (Japan) with the speed of 20 mm/min under the conditions of 25°C and 65 RH.

RESULTS AND DISCUSSION

Two types of composites of ABS and silica, ABS/SiO_2 and ABS—$Si(OCH_3)_3$, were prepared in this study. ABS/SiO_2 was obtained by the formation of hydrogen bonds between cyano groups (—C≡N) in ABS chains and silanol groups of silica networks, while ABS—$Si(OCH_3)_3/SiO_2$ was formed

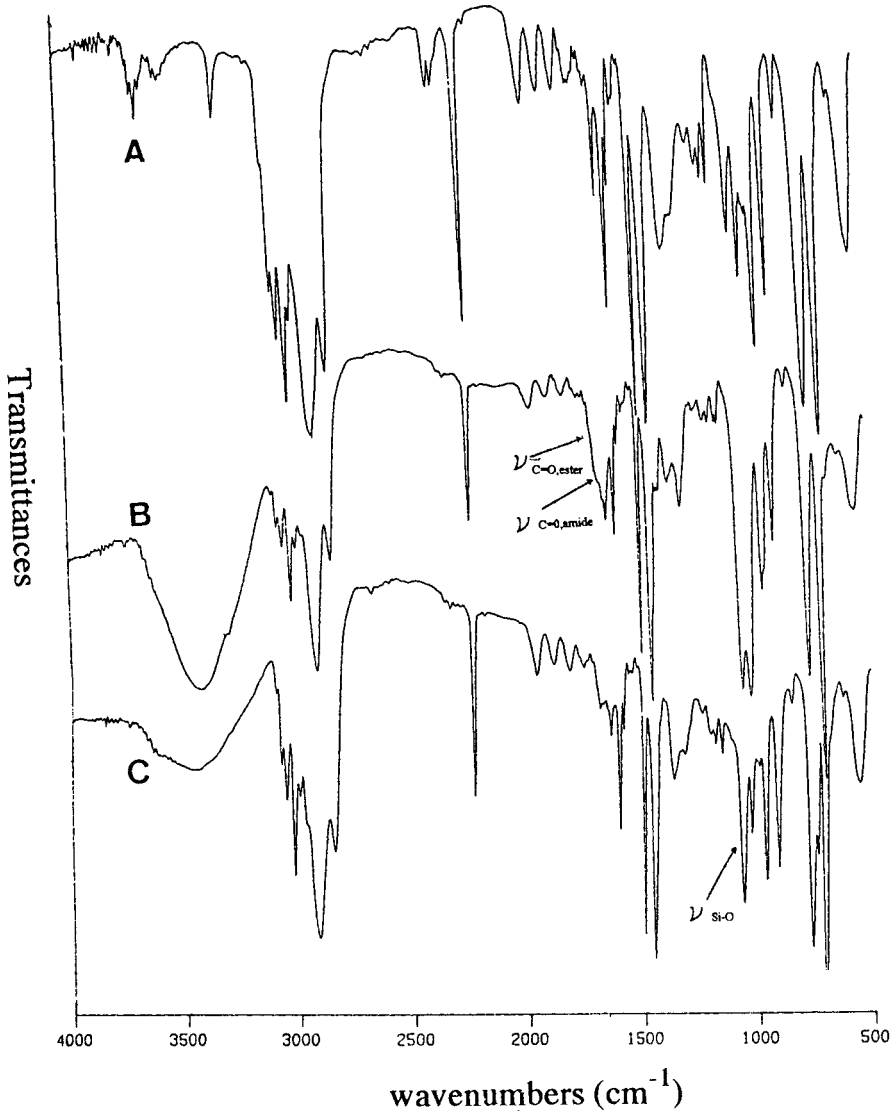

Figure 1 The FTIR spectra of (a) ABS, (b) M-ABS, and (c) ABS—$Si(OCH_3)_3$.

through covalent bonding the ABS chains to the silica network by the sol-gel process of ABS—$Si(OCH_3)_3$ with TEOS. The chemical structure of ABS—$Si(OCH_3)_3$ (Scheme 1) was confirmed by means of IR spectroscopy. Figure 1 showed the FTIR spectra of (a) ABS, (b) M-ABS, and (c) ABS—$Si(OCH_3)_3$. In addition to the characteristic peaks of ABS, the new absorption peaks associated with M-ABS were observed at 1688 cm^{-1}, ($\nu_{C=O\ amide}$), 1704 cm^{-1} ($\nu_{C=O\ acid}$), 3420 cm^{-1} (ν_{-OH}). Similarly, in addition to the characteristic peak of M-ABS, the new absorption peak of ABS—$Si(OCH_3)_3$ was at 1088 cm^{-1} (ν_{Si-O-C}). The other properties of ABS—$Si(OCH_3)_3$ were listed in Table II. It was confirmed that the molecular weight and carbon–carbon double bonds of ABS did not change during the modification reaction of ABS described in Scheme 1.

Gelation of ABS/TEOS and ABS—$Si(OCH_3)_3$/TEOS Sol-Gel Liquid Solutions

It had been pointed out that the microstructure and properties of an oxide gel and the subsequent composite material were governed by numerous interdependent factors, such as the respective properties of the inorganic and organic components (including their chemical compositions, structures, and solubility), the recipes of the sol-gel liquid solution (including the ratio of inor-

Table II Properties of ABS and ABS—$Si(OCH_3)_3$

Polymer	M_w (g/mol)[a]	>=< (mol/kg)[b]	Si (wt %)[c]	$Si(OCH_3)_3$ (mol/kg)
ABS	1.2×10^5	1.74×10^{-2}	0	0
ABS—$Si(OCH_3)_3$	1.3×10^5	1.74×10^{-2}	1.21	0.43

[a] Determined by the GPC.
[b] Quantified by titrating with Wijs reagent.
[c] Determined by thermogravimetric analyzer.

ganic and organic components, water content, solvent, and catalyst species and concentration), and gelation condition (including gelation temperature, atmosphere, and time).[9,10,12–14] In the present study, the chemical structure of the organic polymer was the primary factor. This factor exerted a dramatic effect on the gelation time of the sol-gel liquid solutions.

Figure 2 showed the gelation times of ABS/TEOS and ABS—$Si(OCH_3)_3$/TEOS sol-gel liquid solutions prepared according to the recipes in Table I under the catalyzation of NH_4F. In these systems, the fluoride ion-catalyzed gels exhibited rapid gelation due to nucleophilic substitution of fluoride ion and subsequent rapid hydrolysis and condensation of the reaction site.[9,15] It was found that the gelation times in both solution systems decreased with an increasing catalyst concentration and increased with TEOS content. In ABS—$Si(OCH_3)_3$/TEOS system, because the trimethoxysilyl groups in ABS chains took part in the sol-gel reaction with TEOS and/or ABS—$Si(OCH_3)_3$, it not only formed the covalent bonds with silica but also helped fix the ABS chains in the silica network. Therefore, the gelation time of the system was much shorter than that of the ABS/TEOS system where the ABS chains and silica network were only linked with hydrogen bonding.

Morphology of the Composite Materials

The fractured surfaces of the composite samples, ABS/SiO_2 and ABS—$Si(OCH_3)_3$/SiO_2, obtained, respectively, by further drying the wet gels from sol-gel liquid solutions, ABS/TEOS, and ABS—$Si(OCH_3)_3$/TEOS, were observed by SEM. Important information of the morphology of these composite materials could be deduced in the micrographs. The SEM micrographs in Figure 3 show the microstructures of ABS/SiO_2 and ABS—$Si(OCH_3)_3$/SiO_2 composites under the catalyzation of NH_4F ([NH_4F]/[TEOS] = 0.016 mol ratio), with the silica content of 2.5, 7, and 15 wt %. Figure 3(a) to 3(c) shows the microstructures of the ABS/SiO_2 composites. All micrographs show pores and/or silica particles. Figure 3(d) to 3(f) displays the micrographs of ABS—$Si(OCH_3)_3$/SiO_2 composites; the microstructures were smoother and denser than the ABS/SiO_2 composites with the corresponding silica composition in 3(a) to 3(c). It appeared that the ABS linked with silica by a covalent bond had better compatibility between the two phases than the sample where the two components were connected by hydrogen bonding.[16] Figure 4 is the magnified micrographs of 3(b) and 3(e) (silica content = 7 wt %). It confirmed that the phase of the ABS—$Si(OCH_3)_3$/SiO_2 composite was continuous and without any pores and silica particles on the fracture surface [Fig. 4(a)], while pores and silica particles were found on the fracture surfaces of ABS/SiO_2 com-

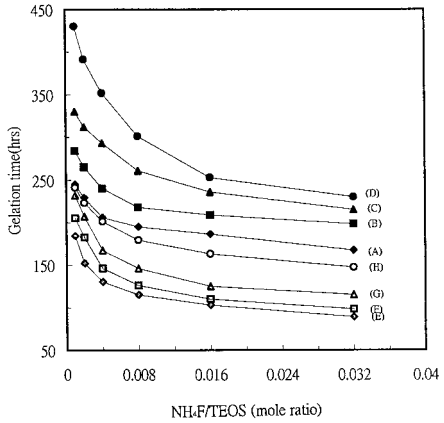

Figure 2 Gelation times of sol-gel liquid solutions, ABS/TEOS, and ABS—$Si(OCH_3)_3$/TEOS, under the catalization of NH_4F of various concentrations. Wt % TEOS in ABS/TEOS: (A) 8.7 (SiO_2 wt % at 2.5); (B) 24.3 (7); (C) 52 (15); (D) 104 (30). Wt % TEOS in ABS—$Si(OCH_3)_3$/TEOS: (E) 8.7 (2.5); (F) 24.3 (7); (G) 52 (15); H,104 (30).

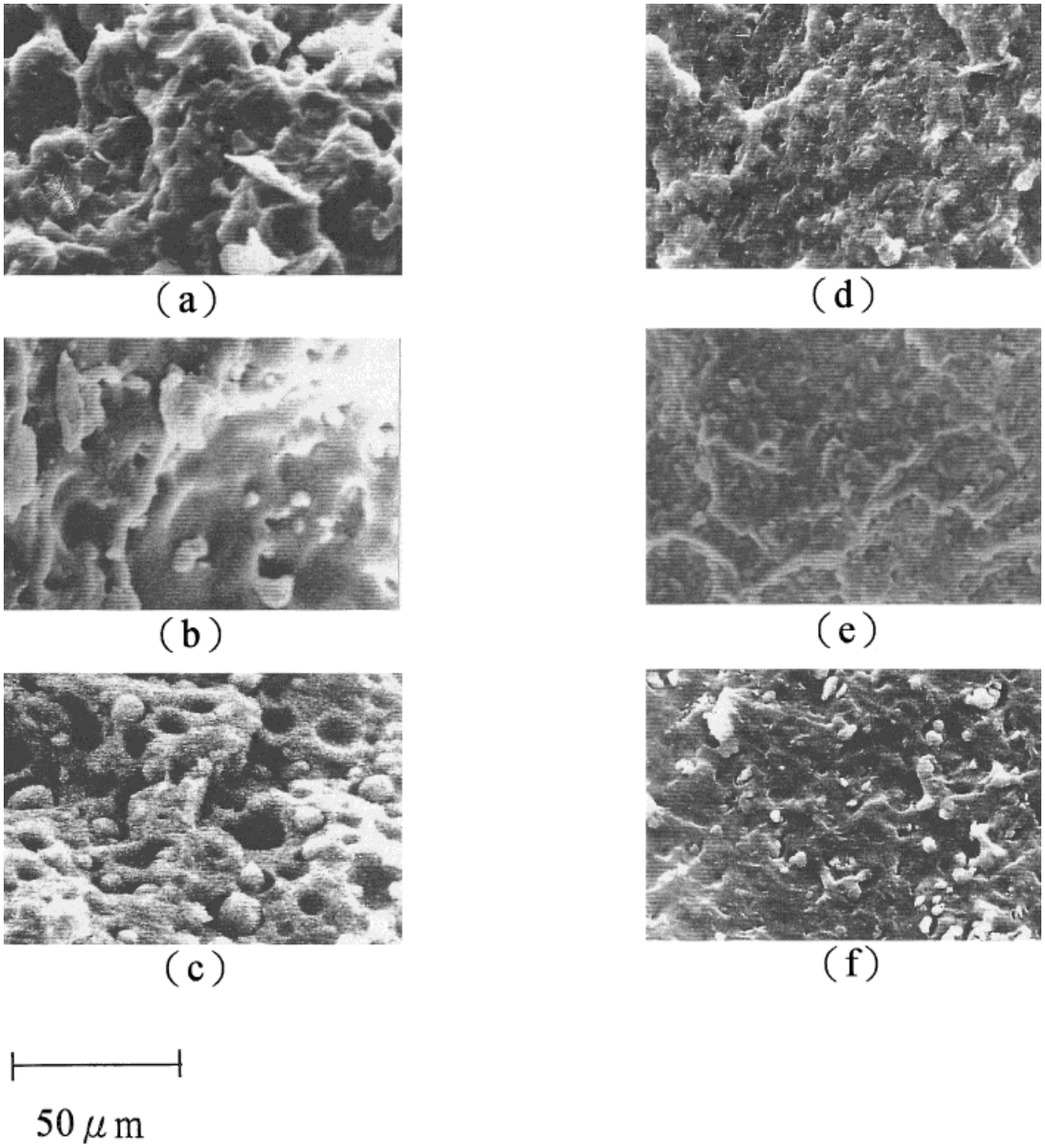

Figure 3 SEM micrographs of the fractured surfaces of ABS/SiO_2 and ABS—$Si(OCH_3)_3/SiO_2$ composites using NH_4F as a catalyst. ABS/SiO_2 with silica content at a wt % of (a) 2.5, (b) 7 and (c) 15. ABS—$Si(OCH_3)_3/SiO_2$ with silica content at a wt % of (d) 2.5, (e) 7, and (f) 15.

posite [Fig. 4(b)]. From the morphology in Figure 3(f) (silica content = 15 wt %) it was found that the glass particles and pores began to appear again on the fractured surface. The morphological observations suggested that the solubility of silica in ABS—$Si(OCH_3)_3/SiO_2$ composites could be obtained with the silica content of or less than 7 wt % for the concentration of —$Si(OCH_3)_3$ in ABS at 0.43 mol/kg under the catalyzation of NH_4F.

DSC Analysis of the Composites

The phase behavior of the composite materials was associated with the cooperative motion of large chain segments (e.g., ABS), which might be hindered by the inorganic metal oxide (silica) network.[11,17] Figure 5 displayed the DSC results of ABS/SiO_2 and ABS—$Si(OCH_3)_3/SiO_2$ composites with the SiO_2 content of 2.5, 7, and 15 wt %. The glass transition temperatures (T_gs) of ABS/SiO_2

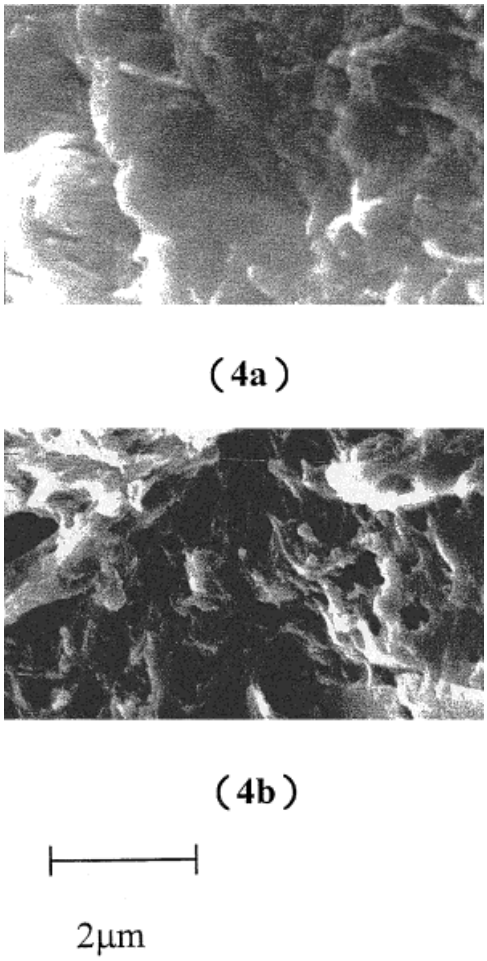

Figure 4 SEM micrographs of fractured surfaces of the (a) ABS—$Si(OCH_3)_3/SiO_2$ and (b) ABS/SiO_2 composites (silica content = 7 wt %), which showed magnified micrographs of Figure 3(b) and 3(e). The phase of the ABS—$Si(OCH_3)_3/SiO_2$ composite was continuous and without any pores and silica particles on the fracture surface, while pores and silica particles were found on the fracture surfaces of the ABS/SiO_2 composite.

composites (curves a to d) shifted only to a slightly higher values (compared with pure ABS) with increasing silica content. Curves e to g were the DSC results of ABS—$Si(OCH_3)_3/SiO_2$ composites. T_gs increased significantly to a higher value with increasing silica content. The T_g reached the highest value when the silica content was ca. 7 wt %. When the silica content was 15 or 30 wt %, the T_g declined with silica content. Increase in T_g of the composites was due to the restriction of ABS chain motion in the composites imposed by the covalent bond between ABS—$Si(OCH_3)_3$ and silica network. The higher the silica content, the larger the restriction of chain motion, and thus the higher the T_g of the composites. However, the T_gs of the composites with the silica content of 15 and 30 wt % were lower than that of the silica content of 7 wt %. This might be due to the presence of excess silica particles [Fig. 3(f)], where some of which might not be linked with the ABS chains through the covalent bond, only dispersed in the ABS matrix. Such particles might cause the separation between the organic and inorganic phases, and deteriorated the compatibility between silica and ABS.[17] Therefore, the T_g of the composites dropped. The T_gs of ABS/SiO_2 and ABS—$Si(OCH_3)_3/SiO_2$ composites were listed in Table III.

Tensile Strength of the Hybrids

Tensile strengths of ABS/SiO_2 and ABS—$Si(OCH_3)_3/SiO_2$ composites were listed in Table III. The tensile strengths could be correlated with the microstructure and phase behavior of the hybrids. Smoother microstructure and a stronger interfacial force of the composites led to higher tensile strength. Therefore, ABS—$Si(OCH_3)_3/SiO_2$ composites exhibited better tensile strength than the ABS/SiO_2 composites with the corresponding composition.

Thermal Stability of the Hybrids

The thermal stabilities of the composites were measured by means of a TGA under nitrogen atmosphere at the heating rate of 10°C min^{-1}. Table III showed the IDT of ABS/SiO_2 and ABS—$Si(OCH_3)_3/SiO_2$ composites. The results in-

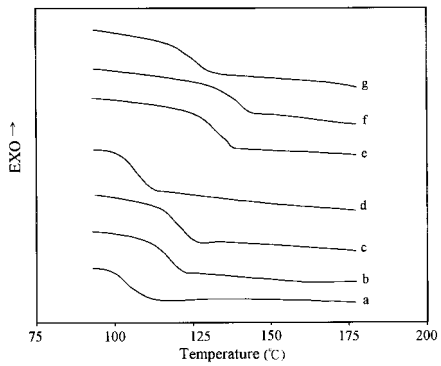

Figure 5 DSC results for the ABS/SiO_2 and ABS—$Si(OCH_3)_3/SiO_2$ composites using NH_4F as a catalyst. ABS/SiO_2 composites with silica content at a wt % of (a) 0 (pure ABS), (b) 2.5, (c) 7, (d) 15, and ABS—$Si(OCH_3)_3/SiO_2$ composites with silica content at a wt % of (e) 2.5, (f) 7, and (g) 15.

Table III Thermal Properties of ABS/SiO_2 and ABS—$Si(OCH_3)_3/SiO_2$ Composites

SiO_2 (wt %)		ABS/SiO_2			ABS—$Si(OCH_3)_3/SiO_2$		
Calc.	Obs.	T_g (°C)	IDT (°C)	TS[a] (MPa)	T_g (°C)	IDT (°C)	TS[a] (MPa)
0	0	107	406	26.3 ± 0.2	106	406	27.3 ± 0.4
2.5	2.6	115	406	35.3 ± 0.8	132	408	45.3 ± 1.1
7	7.8	119	406	41.7 ± 0.8	135	427	50.3 ± 1.2
15	14.6	113	414	30.4 ± 0.5	125	433	35.8 ± 0.9
30	31.5	108	413	24.9 ± 0.3	114	444	27.1 ± 0.6

[a] Tensile strength.

dicated that in ABS/SiO_2 system, the IDT only changed slightly with silica content (Fig. 6). However, the IDT of the ABS—$Si(OCH_3)_3/SiO_2$ composites changed significantly with silica content, where it increased from 406 to 444°C as the content of silica increased from 2.5 to 30%. The enhancement in thermal stability could be attributed to the interaction force between ABS chains and silica network, and the consequential uniform distribution of the silica in the ABS matrix.[19,20] In the ABS/SiO_2 composites systems, because the intermolecular force between ABS and silica was the weaker hydrogen bonding, the distribution of silica in the ABS polymer matrix was not very even [see Fig. 3(a) to 3(c)], and thus the increase in IDT was not significant. For the ABS—$Si(OCH_3)_3/SiO_2$ composite systems, because the ABS chains and the silica network were linked by covalent bonds, the distribution of silica in the ABS polymer matrix was more uniform; therefore, the thermal stability of the composites was significantly enhanced with the silica content.

CONCLUSIONS

Organic–inorganic composites materials had been prepared by an *in situ* sol-gel process of TEOS in the presence of ABS and ABS—$Si(OCH_3)_3$, obtained by oxidizing the cyano group in ABS with hydrogen peroxide, which subsequently underwent ring-opening reaction with GPTS, under the catalization of NH_4F. In the ABS—$Si(OCH_3)_3$/TEOS sol-gel liquid solution system the ABS chains formed the covalent bonds with a silica network, and helped fix the polymer chains in the silica network. Therefore, the gelation time of this system was much shorter than that of ABS/TEOS system, which linked ABS chains and silica network only by hydrogen bonding the cyano groups in ABS to the silanol groups.

The microstructural morphologies of the composites, ABS/SiO_2 and ABS—$Si(OCH_3)_3/SiO_2$, were observed by SEM. In the ABS/SiO_2 composite, obvious pores and interfaces between silica particles and the polymer matrix were observed. In the ABS—$Si(OCH_3)_3/SiO_2$ composite, however, the introduction of covalent bonding created smoother and denser microstructures. The composites displayed continuous phases with no particles and pores when the silica content was ca. 2.5 and 7 wt %.

The T_gs of ABS/SiO_2 composite, in which ABS was not chemically bonded to the silica network,

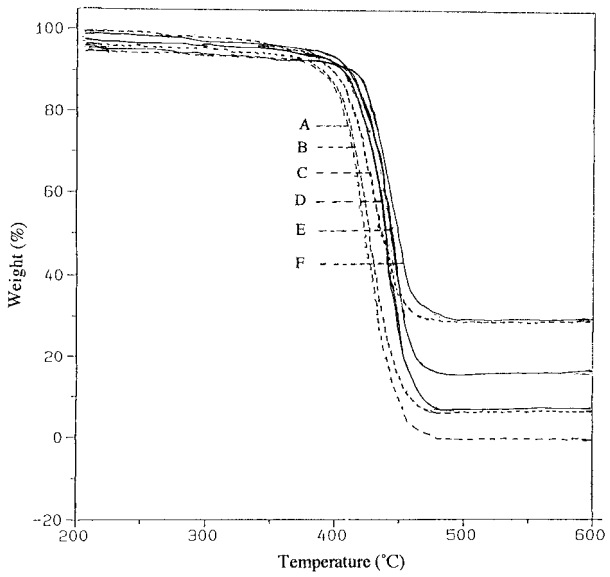

Figure 6 TGA curves for ABS/SiO_2 and ABS—$Si(OCH_3)_3/SiO_2$ composites with various silica content at a heating rate of 10°C/min in N_2. ABS/SiO_2 hybrids (dashed line) with silica content at a wt % of (A) 0 (pure ABS), (B) 7, and (C) 30, and ABS—$Si(OCH_3)_3/SiO_2$ hybrids (solid line) with silica content at a wt % of (D) 7, (E) 15, and (F) 30.

were only slightly higher than that of pure ABS, which was consistent, with relatively weak hydrogen bonding between the organic and inorganic phases. However, in the ABS—$Si(OCH_3)_3/SiO_2$ composite, in which the ABS matrix linked to the silica network with covalent bonds, the increase in T_g was much higher because of the better cohesion between the phases and large reduction in segmental mobility of the ABS. The highest value of T_g (135°C) was observed for the composites with the silica content of 7 wt %. Tensile strength was found to correlate well with the microstructure and phase behavior of the composite. Smoother microstructure and stronger interfacial force led to stronger tensile strength. Therefore, ABS—$Si(OCH_3)_3/SiO_2$ composites of every silica content were stronger than that of corresponding ABS/SiO_2 composites.

The enhancement in thermal stability of the composites could be attributed to the interaction force between ABS chains and silica network, and the content of silica in the composites. The IDT of ABS/SiO_2 composites with various silica contents were similar to that of pure ABS, while in the ABS—$Si(OCH_3)_3/SiO_2$ composites, the IDT greatly increased with silica content.

The authors wish to express their thanks to the National Science Council for financial support under the grant No. NSC-86-2216-E-011-022, and to Dr. H. L. Chen for his help with the manuscript.

REFERENCES

1. Schmidt, H. J Noncryst Solids 1985, 73, 681.
2. Mark, J. E.; Lee, C. Y.-C.; Bianconi, P. A., Eds., Hybrid Organic–Inorganic Composite; American Chemical Society: Washington, DC, 1995.
3. Novak, B. M. Adv Mater 1993, 5, 422.
4. Huang, H.; Glaser, R. H.; Wilkes, G. L. Macromolecules 1987, 20, 1322.
5. Wilkes, G. L.; Wen, J. In Polymeric Materials Encyclopedia: Salamone, J. C., Editor-in chief; CRC Press: New York, 1996; p 2782, Vol. 6.
6. Allcock, H. R. In Chemical Processing of Advanced Materials; Hench, L. L.; West, J. K., Eds.; Wiley & Son: New York, 1992.
7. Saegusa, T. Pure Appl Chem 1995, 67, 1965.
8. Schmidt, H., et al. In Ultra-Structure Processing of Advanced Ceramics; Mackenzie, J. K.; Urick, D. R., Eds.; John Wiley: New York, 1988.
9. Pope, E. J. A.; Mackenzie, J. D. J Noncryst Solids 1986, 81, 148.
10. Brennan, A. B.; Wilkes, G. L. Polymer 1991, 32, 733.
11. Wei, Y.; Wang, W.; Yang, D.; Tang, L. Chem Mater 1994, 6, 1737.
12. Hsu, Y. G.; Huang, J. H. J Noncryst Solids 1996, 208, 259.
13. Brinker, C. J., et al. J Noncryst Solids 1984, 63, 45.
14. Mackenzie, J. D.; Chung, Y. J.; Hu, Y. J Noncryst Solids 1992, 147, 271.
15. Cerveau, G., et al. In Hybrid Organic–Inorganic Composite; Mark, J. E.; Lee, C. Y.-C.; Bianconi, P. A., Eds.; American Chemical Society: Washington, DC, 1995; p. 210.
16. Huang, Z. H.; Qiu, K. Y. Polymer 1997, 38, 521.
17. Huang, Z. H.; Qiu, K. Y.; Wei, Y. J Polym Sci Part A Polym Chem 1997, 36, 2403.
18. Ahmad, Z.; Sarwar, M. I.; Mark, J. E. J Appl Polym Sci 1997, 63, 1345.
19. Wang, S.; Ahmad, Z.; Mark, J. E. Polym Bull 1993, 31, 323.
20. Wei, Y.; Yang, D.; Bakthvatchalam, R. Mater Lett 1992, 13, 261.